Decoherence and degradation of squeezed states in quantum filter cavities

P. Kwee, J. Miller,* T. Isogai, L. Barsotti, and M. Evans

LIGO Laboratory, Massachusetts Institute of Technology, 185 Albany Street, Cambridge, Massachusetts 02139, USA

(Received 17 March 2014; published 5 September 2014)

Squeezed states of light have been successfully employed in interferometric gravitational-wave detectors to reduce quantum noise, thus becoming one of the most promising options for extending the astrophysical reach of the generation of detectors currently under construction worldwide. In these advanced instruments, quantum noise will limit sensitivity over the entire detection band. Therefore, to obtain the greatest benefit from squeezing, the injected squeezed state must be filtered using a long-storage-time optical resonator, or "filter cavity," so as to realize a frequency-dependent rotation of the squeezed quadrature. While the ultimate performance of a filter cavity is determined by its storage time, several practical decoherence and degradation mechanisms limit the experimentally achievable quantum noise reduction. In this paper we develop an analytical model to explore these mechanisms in detail. As an example, we apply our results to the 16 m filter cavity design currently under consideration for the Advanced LIGO interferometers.

DOI: 10.1103/PhysRevD.90.062006 PACS numbers: 04.80.Nn, 42.50.Dv, 04.30.-w, 42.50.Lc

I. INTRODUCTION

Squeezed states of light are used in a variety of experiments in optical communication, biological sensing and precision measurement [1–3]. To gravitational-wave detectors, the finest position-meters ever built, squeezed states of light today represent one of the most mature technologies for further expanding the detectable volume of the universe [4,5].

The advanced detectors currently under construction, such as Advanced LIGO [6], will be limited by quantum noise over their entire detection band, from 10 Hz to 10 kHz. To fully exploit the potential of squeezing, squeezed states must therefore be manipulated so as to impress a frequency-dependent rotation upon the squeezing ellipse. Such rotation can be realized by reflecting the squeezed states from a detuned, over-coupled, optical resonator, called a quantum filter cavity.

The performance of ideal filter cavities, fundamentally limited by their storage times, is well-understood [7,8] and a proof-of-principle experimental demonstration has been performed [9]. However, the impact of several decoherence and degradation mechanisms which critically determine the achievable performance of astrophysically relevant filter cavities has not yet been investigated.

In this paper we present an analytical model, based on the two-photon formalism [10–12], which evaluates the reduction in observable squeezing caused by optical losses and by spatial mode mismatch between the injected squeezed light, the filter cavity and the interferometer. Further, we also explore the influence of squeezed quadrature fluctuations [13], or "phase noise," generated both inside and outside the filter cavity. As a concrete example, we study the effects of these noise sources on a 16 m long filter cavity with a 60 Hz linewidth, parameters considered for Advanced LIGO [14].

II. ANALYTICAL MODEL

The frequency-dependent squeezing system modelled in this work is shown in Fig. 1. The squeezed beam is injected into the interferometer after reflection from the filter cavity. In this model we assume that the quantum noise enhancement is measured via a generic homodyne readout system, by beating the interferometer output field against a local oscillator (LO) field. The main sources of squeezing decoherence (optical loss and mode mismatch) and degradation (phase noise due to local-oscillator phase-lock errors and cavity length fluctuations) are indicated.

Using the mathematical formalism described in [14] and further developed in Appendix A, our analysis calculates the achievable quantum noise reduction by propagating three classes of vacuum field through the optical system: v_1 which passes through the squeezer and becomes the squeezed field; v_2 which accounts for all vacuum fluctuations that are coupled into the beam due to optical losses *before* the interferometer; and v_3 which accounts for vacuum fluctuations introduced due to losses *after* the interferometer. In this formalism vacuum fields are proportional to the identity matrix, $v_1 = v_2 = v_3 = \sqrt{2\hbar\omega_0}\mathbf{I}$, and their interaction with an optical element or system may be described by multiplication with a 2×2 transmission matrix $\mathbf{T}$, i.e. $v_{\mathrm{out}} = \mathbf{T}v_{\mathrm{in}}$.

In Secs. II A, II B and II C we develop transfer matrices for the propagation of v_1 through the squeezer and injection optics, its modification by the filter cavity and the influence

*jmiller@ligo.mit.edu

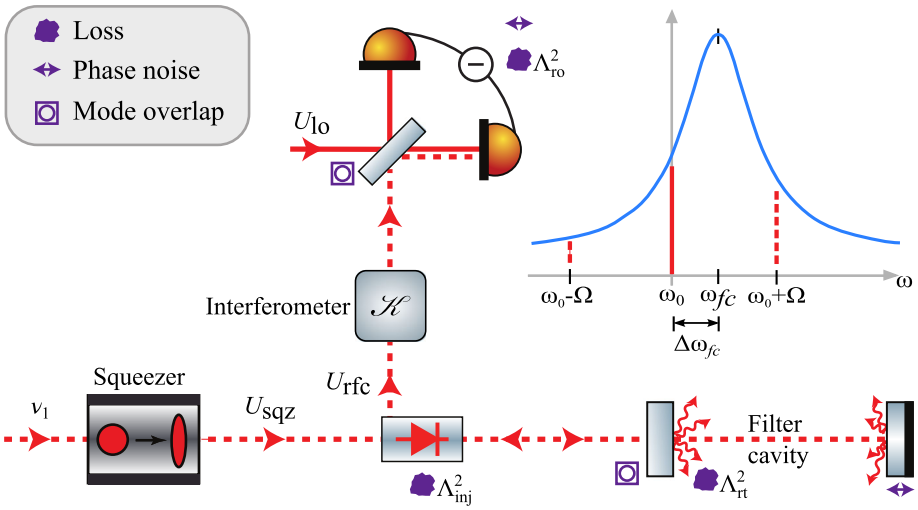

FIG. 1 (color online). The frequency-dependent squeezing system analyzed in this work. The squeezer generates a frequency-independent squeezed state with spatial mode $U_{\rm sqz}$. The squeezed state becomes frequency dependent after reflection from a filter cavity and is subsequently detected via homodyne readout using a local oscillator with spatial mode $U_{\rm lo}$.

it experiences due to imperfect mode matching. Section II D constructs a transfer matrix describing the optomechanical coupling of the interferometer and shows that it can be written as a product of rotation and squeezing operators. We then, in Sec. II E, incorporate the uncontrolled vacuum noise coupled into the squeezed field due to loss and show how one can compute the quantum noise at the readout of the interferometer using the matrices developed in the previous sections. The final piece of our analytical model, performance degradation due to phase noise, is detailed in Sec. II F.

A. Squeezed field injection

The squeezer is represented by the operator $\mathbf{S}(\sigma,\phi)$, given by

$$\mathbf{S}(\sigma,\phi)=\mathbf{R}(\phi)\mathbf{S}(\sigma,0)\mathbf{R}(-\phi)=\mathbf{R}_\phi\mathbf{S}_\sigma\mathbf{R}_\phi^\dagger = \begin{pmatrix}\cos\phi & -\sin\phi\\ \sin\phi & \cos\phi\end{pmatrix}\begin{pmatrix}e^{\sigma} & 0\\ 0 & e^{-\sigma}\end{pmatrix}\begin{pmatrix}\cos\phi & \sin\phi\\ -\sin\phi & \cos\phi\end{pmatrix}, \tag{1}$$

which describes squeezing by $e^{-\sigma}$ at angle ϕ and antisqueezing by e^{σ} at $\phi+\pi/2$. Conventionally, squeezing magnitudes are expressed in decibels (dB), with $\sigma_{\rm dB}=\sigma\times 20\log_{10}e$.

In general, all optical losses outside of the filter cavity are frequency independent or the frequency dependence is so small that it can be neglected. Examples of optical losses are residual transmissions of steering mirrors, scattering, absorption and imperfections in polarization optics. The last of these is likely to dominate the frequency-independent losses incurred in the passage of the squeezed field to the readout, therefore these losses are represented in Fig. 1 as occurring at the optical isolator.

Since there are no nonlinear elements in our system between the squeezer and the interferometer (i.e. nothing which mixes upper and lower audio sidebands) we can combine all of the input losses together into a single frequency-independent "injection loss", $\Lambda^2_{\rm inj}$, which represents the total power loss outside of the filter cavity and before the readout (this work does not consider any losses within the interferometer itself).

Amalgamating the losses with the action of the squeezer, we arrive at the two-photon transfer matrix which takes v_1 to the filter cavity [15],

$$\mathbf{T_{inj}}=\tau_{\rm inj}\mathbf{S}(\sigma_{\rm sqz},\phi_{\rm sqz}), \tag{2}$$

where the attenuation due to $\Lambda^2_{\rm inj}$ is described by the transfer coefficient $\tau_{\rm inj}=\tau(\Lambda_{\rm inj})=\sqrt{1-\Lambda^2_{\rm inj}}$.

B. Filter cavity

Reflection from a filter cavity is a linear process which can easily be described in the one-photon, and therefore two-photon, formalisms, as in equation (A9) of [14]. However, the approach therein does not permit one to explore the consequences of filter cavity imperfections analytically, with resulting loss of physical insight. Here we revisit this equation and, by making appropriate approximations, construct a closed-form expression for the action of a filter cavity in the two-photon formalism.

For a given signal sideband frequency Ω, the complex reflectivity, $r_{\rm fc}(\Omega)$, of a filter cavity, using the same notation as [14], is given by

$$r_{\rm fc}(\Omega) = r_{\rm in} - \frac{t_{\rm in}^2}{r_{\rm in}} \frac{r_{\rm rt} e^{-i\Phi(\Omega)}}{1 - r_{\rm rt} e^{-i\Phi(\Omega)}}, \tag{3}$$

where $r_{\rm in}$ is the amplitude reflectivity of the input mirror and $r_{\rm rt}$ is the cavity's round-trip amplitude reflectivity. For a cavity of length $L_{\rm fc}$ and resonant frequency $\omega_{\rm fc}$, the round-trip phase $\Phi(\Omega)$ is defined as

$$\Phi(\Omega) = (\Omega - \Delta\omega_{\rm fc}) \frac{2L_{\rm fc}}{c}, \tag{4}$$

where $\Delta\omega_{\rm fc} = \omega_{\rm fc} - \omega_0$ is the cavity detuning with respect to the carrier frequency ω_0 and c is the speed of light.

For a high-finesse cavity near to resonance, we can make the approximations

$$e^{-i\Phi(\Omega)} \simeq 1 - i\Phi(\Omega) \tag{5}$$

and

$$r_{\rm rt} \simeq r_{\rm in} \simeq \sqrt{1 - t_{\rm in}^2 - \Lambda_{\rm rt}^2} \simeq 1 - (t_{\rm in}^2 + \Lambda_{\rm rt}^2)/2, \tag{6}$$

where $\Lambda_{\rm rt}^2$ accounts for the power lost during one round-trip in the cavity (not including input mirror transmission).

Under these approximations, and neglecting terms of order 1 or greater in $\Lambda_{\rm rt}^2$, $t_{\rm in}^2$ and $\Phi(\Omega)$, (3) can be rewritten as [16]

$$r_{\rm fc}(\Omega) = 1 - \frac{2 - \epsilon}{1 + i\xi(\Omega)} = \frac{\epsilon - 1 + i\xi(\Omega)}{1 + i\xi(\Omega)}, \tag{7}$$

where

$$\epsilon = \frac{2\Lambda_{\rm rt}^2}{t_{\rm in}^2 + \Lambda_{\rm rt}^2} = \frac{c\Lambda_{\rm rt}^2}{2L_{\rm fc}\gamma_{\rm fc}} = \frac{f_{\rm FSR}}{\gamma_{\rm fc}} \Lambda_{\rm rt}^2, \tag{8}$$

$$\xi(\Omega) = \frac{2\Phi(\Omega)}{t_{\rm in}^2 + \Lambda_{\rm rt}^2} = \frac{\Omega - \Delta\omega_{\rm fc}}{\gamma_{\rm fc}} \tag{9}$$

and the cavity half-width-half-maximum-power linewidth is defined as

$$\gamma_{\rm fc} = \frac{1 - r_{\rm rt}^2}{2} \frac{c}{2L_{\rm fc}} = \frac{t_{\rm in}^2 + \Lambda_{\rm rt}^2}{2} \frac{c}{2L_{\rm fc}}. \tag{10}$$

As noted by previous authors [17], for a given cavity half-width $\gamma_{\rm fc}$, the filter cavity performance is determined entirely by the loss per unit length $\Lambda_{\rm rt}^2/L_{\rm fc}$.

To investigate the effect the filter cavity has on a squeezed field we must convert its response, (7), into the two-photon picture. This is done with the one-photon to two-photon conversion matrix (see [14] and Sec. A 3),

$$\mathbf{A_2} = \frac{1}{\sqrt{2}} \begin{pmatrix} 1 & 1 \\ -i & +i \end{pmatrix}, \tag{11}$$

yielding the transfer matrix

$$\mathbf{T_{fc}} = \mathbf{A_2} \cdot \begin{pmatrix} r_+ & 0 \\ 0 & r_-^* \end{pmatrix} \cdot \mathbf{A_2}^{-1}, \tag{12}$$

where $r_\pm = r_{\rm fc}(\pm\Omega)$.

To cast this expression in a more instructive form, we require several sum and difference quantities based on $r_{\rm fc}(\Omega)$. In terms of ϵ and $\xi(\Omega)$, the complex phase and magnitude of $r_{\rm fc}(\Omega)$ are given by

$$\begin{aligned} \alpha_{\rm fc}(\Omega) &= \arg(r_{\rm fc}(\Omega)) \\ &= \arg(-1 + \epsilon + \xi^2(\Omega) + i(2 - \epsilon)\xi(\Omega)) \end{aligned} \tag{13}$$

and

$$\rho_{\rm fc}(\Omega) = |r_{\rm fc}(\Omega)| = \sqrt{1 - \frac{(2 - \epsilon)\epsilon}{1 + \xi^2(\Omega)}}, \tag{14}$$

whence we define

$$\begin{aligned} &\alpha_\pm = \alpha_{\rm fc}(\pm\Omega), \qquad \rho_\pm = \rho_{\rm fc}(\pm\Omega), \\ &\alpha_{\substack{p \\ m}} = \frac{\alpha_+ \pm \alpha_-}{2} \quad \text{and} \quad \rho_{\substack{p \\ m}} = \frac{\rho_+ \pm \rho_-}{2}, \end{aligned} \tag{15}$$

where the subscripts p and m are used to denote the sum and difference of the phases and magnitudes.

The transfer matrix of the filter cavity can then be expressed in a form which clearly shows the effect of intracavity loss,

$$\mathbf{T_{fc}} = \underbrace{e^{i\alpha_m} \mathbf{R}_{\alpha_p}}_{\text{lossless}} \underbrace{(\rho_p \mathbf{I} - i\rho_m \mathbf{R}_{\pi/2})}_{\text{lossy}}, \tag{16}$$

where $\mathbf{I}$ is the 2×2 identity matrix.

The first term in this expression, marked "lossless," consists of a rotation operation and an overall phase which are identical to the rotation and phase provided by a lossless filter cavity [7].

The second, "lossy", term goes to unity for a lossless filter cavity ($\rho_p = 1$ and $\rho_m = 0$). However, in the presence of losses, this term mixes the quadratures of the squeezed state, corrupting squeezing with antisqueezing. We emphasize that this effect is not *decoherence*, as we have not yet introduced the vacuum fluctuations which enter as a consequence of the filter cavity losses, but rather a *coherent dephasing* of the squeezed quadratures which cannot be undone by rotation of the state. This dephasing is a direct result of different reflection magnitudes experienced by the upper and lower audio sidebands (i.e. $\rho_m \neq 0$). The

ramifications of this effect on the measured noise are presented in Sec. II E.

Additionally, by combining (13) and (15), we are now able to write an explicit expression for the squeezed quadrature rotation, α_p, produced by the filter cavity,

$$\alpha_p \simeq \mathrm{atan}\left(\frac{(2-\epsilon)\gamma_{\mathrm{fc}}\Delta\omega_{\mathrm{fc}}}{(1-\epsilon)\gamma_{\mathrm{fc}}{}^2 - \Delta\omega_{\mathrm{fc}}{}^2 + \Omega^2}\right), \tag{17}$$

which holds for typical filter cavity parameters, $\epsilon \ll 1 \Rightarrow \Lambda_{\mathrm{rt}}^2 \ll t_{\mathrm{in}}^2$. In particular, for a lossless filter cavity ($\epsilon = 0$),

$$\alpha_p = \mathrm{atan}\left(\frac{2\gamma_{\mathrm{fc}}\Delta\omega_{\mathrm{fc}}}{\gamma_{\mathrm{fc}}{}^2 - \Delta\omega_{\mathrm{fc}}{}^2 + \Omega^2}\right), \tag{18}$$

consistent with the expression for α_p which can be deduced from (88) of [7] (note that the referenced equation is missing factor of 2, as reported in [8]).

C. Mode matching

A quantum filter cavity modifies the phase of the squeezed state which is coupled into its resonant mode. In a laboratory context, free-space optics are used to perform this coupling, maximizing the spatial overlap between the cavity mode and the incident beam. This process is known as "mode matching" and the result is inevitably imperfect. In the case of quantum filter cavities, imperfect mode matching results in both a source of loss and in a path by which the squeezed state can bypass the filter cavity. In this section we develop a model describing how imperfect filter cavity mode matching affects a squeezed state. Furthermore, we also include the effects of loss arising from mode mismatch between the squeezed field and the beam, known as the "local oscillator" (LO), used to detect it.

The previously stated filter cavity reflectivity r_{fc} applies only to a field perfectly mode matched to the cavity fundamental mode. In order to incorporate mode mismatch, we express the LO and the beam from the squeezed light source in an orthonormal basis of spatial modes U_n (e.g. Hermite-Gauss or Laguerre-Gauss modes) such that

$$U_{\mathrm{sqz}} = \sum_{n=0}^{\infty} a_n U_n, \quad \text{with} \quad a_0 = \sqrt{1 - \sum_{n=1}^{\infty} |a_n|^2} \tag{19}$$

$$U_{\mathrm{lo}} = \sum_{n=0}^{\infty} b_n U_n, \quad \text{with} \quad b_0 = \sqrt{1 - \sum_{n=1}^{\infty} |b_n|^2} \tag{20}$$

where a_n and b_n are complex coefficients. We further choose this basis such that U_0 is the filter cavity fundamental mode. For $a_0 = 1$ the beam from the squeezed light source is perfectly matched to the filter cavity mode. Similarly, $b_0 = 1$ indicates that the local oscillator beam has perfectly spatial overlap with the filter cavity mode.

Since the filter cavity is held near the resonance of the fundamental mode, we assume that all other modes (U_n with $n > 0$) are far from resonance, with $\xi \gg 1$ and $r_{\mathrm{fc}} \simeq 1$. Thus, the squeezed beam after reflection from the filter cavity is given by

$$U_{\mathrm{rfc}} = r_{\mathrm{fc}}(\Omega) \cdot U_{\mathrm{sqz}} = r_{\mathrm{fc}}(\Omega) a_0 U_0 + \sum_{n=1}^{\infty} a_n U_n. \tag{21}$$

The fundamental mode's amplitude and phase are modified by the filter cavity, whereas those of the other modes remain unchanged since these modes are not resonant and the filter cavity acts like a simple mirror.

The spatial overlap integral of the reflected field U_{rfc} and the local oscillator U_{lo} is

$$\langle U_{\mathrm{lo}} | U_{\mathrm{rfc}} \rangle = t_{00} r_{\mathrm{fc}}(\Omega) + t_{\mathrm{mm}} \tag{22}$$

where $t_{00} = a_0 b_0^*$ and $t_{\mathrm{mm}} = \sum_{n=1}^{\infty} a_n b_n^*$. Note that t_{mm} represents the overlap between the mismatched part of the beam from the squeezed light source and the mismatched LO. The squeezed field which follows this path essentially bypasses the filter cavity, and thereby *experiences no frequency-dependent rotation*. It may, however, acquire a frequency-independent rotation with respect to the field which couples into the filter cavity, as can be seen from the two-photon mode-mismatch matrix,

$$\mathbf{T_{mm}} = \mathbf{A_2} \cdot \begin{pmatrix} t_{\mathrm{mm}} & \\ & t_{\mathrm{mm}}^* \end{pmatrix} \cdot \mathbf{A_2}^{-1} = |t_{\mathrm{mm}}| \mathbf{R}(\arg(t_{\mathrm{mm}})). \tag{23}$$

The addition of this coupling path results in a frequency-dependent rotation error with respect to the rotation expected from a perfectly mode matched filter cavity. For modest amounts of mode mismatch (less than 10%), this error can be corrected by a small change in the filter cavity detuning.

The magnitude of the mode mismatch is constrained by t_{00} such that

$$|t_{\mathrm{mm}}| \leq \sqrt{(1-a_0^2)(1-b_0^2)} \leq 1 - t_{00} \tag{24}$$

while the phase is in general unconstrained. The $\langle U_{\mathrm{lo}} | U_{\mathrm{rfc}} \rangle$ overlap is maximized when t_{mm} is real and positive and minimized when it is real and negative.

Experimentally, the quantities which one can easily measure are the squeezed field/filter cavity power mode-coupling, a_0^2, and the squeezed field/local oscillator power mode-coupling, c_0^2, say. From these values one can determine b_0, the overlap between the LO and filter cavity modes, in the following way,

$$b_0 = \langle U_{\rm lo}|U_0\rangle = a_0 c_0 + \sqrt{(1-a_0^2)(1-c_0^2)}\exp(i\phi_{\rm mm}), \tag{25}$$

where $\phi_{\rm mm}$ captures the ambiguity in the $t_{\rm mm}$ phase. The parameters of interest for noise propagation are then easily determined,

$$t_{00} = a_0 b_0^*, \tag{26}$$

$$t_{\rm mm} = c_0 - t_{00}. \tag{27}$$

Note that the second equality in (25) is not universally true. The magnitude of the second term (the expression multiplying the exponential) can be smaller than that given, depending on the unknown character of the mode mismatches. However this choice, an upper bound, allows one to explore the full range of b_0 values necessary to constrain the mode-mismatch-induced noise.

D. Interferometer

The nonlinear action of radiation pressure in an interferometer affects any vacuum field incident upon it. In our analysis, we include an idealized lossless interferometer to illustrate this phenomenon. Operated on resonance, such an interferometer may be described by the transfer matrix

$$\mathbf{T_{ifo}} = \begin{pmatrix} 1 & 0 \\ -\mathcal{K} & 1 \end{pmatrix}, \tag{28}$$

as reported in [18]. Here, $\mathcal{K}$ characterizes the coupling of amplitude fluctuations introduced at the interferometer's dark port to phase fluctuations exiting the same port and takes the form

$$\mathcal{K} = \left(\frac{\Omega_{\rm SQL}}{\Omega}\right)^2 \frac{\gamma_{\rm ifo}^2}{\Omega^2 + \gamma_{\rm ifo}^2}, \tag{29}$$

where $\gamma_{\rm ifo}$ is the interferometer signal bandwidth and $\Omega_{\rm SQL}$ is a characteristic frequency, dependent on the particular interferometer configuration, which approximates the frequency at which the interferometer quantum noise equals the standard quantum limit (i.e. where radiation pressure noise intersects shot noise [7]).

For a conventional interferometer without a signal recycling mirror, like the power-recycled Michelson interferometer described in [7],

$$\gamma_{\rm ifo_0} = \gamma_{\rm arm} \simeq \frac{T_{\rm arm} c}{4 L_{\rm arm}} \tag{30}$$

and

$$\Omega_{\rm SQL_0} \simeq \frac{8}{c}\sqrt{\frac{P_{\rm arm}\omega_0}{m T_{\rm arm}}}, \tag{31}$$

where $P_{\rm arm}$ is the laser power stored inside the interferometer arm cavities, ω_0 is the frequency of the carrier field, $L_{\rm arm}$ is the arm cavity length, m is the mass of each test mass mirror, $T_{\rm arm}$ is the power transmissivity of the arm cavity input mirrors and approximations are valid provided arm cavity finesse is high.

For a dual-recycled interferometer, operating with a tuned signal-recycling cavity of length $L_{\rm src}$, it can be shown that, for $\Omega \ll c/L_{\rm src}$,

$$\gamma_{\rm ifo} = \frac{1+r_{\rm sr}}{1-r_{\rm sr}}\gamma_{\rm ifo_0} \tag{32}$$

and

$$\Omega_{\rm SQL} = \frac{t_{\rm sr}}{1+r_{\rm sr}}\Omega_{\rm SQL_0}, \tag{33}$$

where $t_{\rm sr}$ and $r_{\rm sr}$ are the amplitude transmissivity and reflectivity of the signal recycling mirror. Given the Advanced LIGO parameters reported in Table I,

$$\gamma_{\rm ifo} \simeq 9\gamma_{\rm ifo_0} \simeq 2\pi \times 390\ {\rm Hz} \tag{34}$$

and

$$\Omega_{\rm SQL} \simeq \frac{\Omega_{\rm SQL_0}}{3} \simeq 2\pi \times 70\ {\rm Hz}, \tag{35}$$

confirming that the effect of signal recycling in Advanced LIGO is to increase the interferometer's bandwidth while reducing the frequency at which its quantum noise reaches the SQL. For such an interferometer, in which $\gamma_{\rm ifo} \gg \Omega_{\rm SQL}$, $\mathcal{K}$ may be approximated by $(\Omega_{\rm SQL}/\Omega)^2$ in the region of interest (where $\mathcal{K}$ is order unity or larger).

While (28) is very simple, greater appreciation of the action of the interferometer can be gained by noting that

TABLE I. Symbols and values for aLIGO interferometer parameters.

Parameter	Symbol	Value
Frequency of the carrier field	ω_0	$2\pi \times 282$ THz
Arm cavity length	L	3995 m
Signal recycling cavity length	$L_{\rm src}$	55 m
Arm cavity half-width	$\gamma_{\rm arm}$	$2\pi \times 42$ Hz
Arm cavity input mirror power transmissivity	$T_{\rm arm}$	1.4%
Signal recycling mirror power transmissivity	$t_{\rm sr}^2$	35%
Intracavity power	$P_{\rm arm}$	800 kW
Mass of each test mass mirror	m	40 kg

$\mathbf{T_{ifo}}$ can be recast in terms of the previously defined squeeze and rotation operators as

$$\mathbf{T_{ifo}} = \mathbf{S}(\sigma_{\rm ifo}, \phi_{\rm ifo})\mathbf{R}(\theta_{\rm ifo}) \tag{36}$$

with

$$\begin{aligned}\sigma_{\rm ifo} &= -\,\text{arcsin}\,h(\mathcal{K}/2),\\ \phi_{\rm ifo} &= \frac{1}{2}\text{arccot}(\mathcal{K}/2),\\ \theta_{\rm ifo} &= -\,\text{arctan}(\mathcal{K}/2).\end{aligned}$$

The role of the filter cavity is to rotate the input squeezed quadrature as a function of frequency such that it is always aligned with the signal quadrature at the output of the interferometer, even in the presence of rotation by $\theta_{\rm ifo}$ and the effective rotation caused by squeezing at angle $\phi_{\rm ifo}$. The required filter cavity rotation is given by

$$\theta_{\rm fc} = \text{arctan}(\mathcal{K}). \tag{37}$$

E. Linear noise transfer

We now combine the intermediate results of previous sections to compute the quantum noise observed in the interferometer readout. Three vacuum fields make contributions to this noise: v_1 which passes through the squeezer, v_2 which enters before the interferometer but does not pass through the squeezer and v_3 which enters after the interferometer. We formulate transfer matrices for each of these fields in turn before providing, in (43), a final expression for the measured noise.

Converting the result of (22) into a two-photon transfer matrix and including losses in the injection and readout paths, via $\mathbf{T_{inj}}$ and $\tau_{\rm ro}$ respectively [see (2) and (42)], we arrive at the full expression describing the transfer of vacuum field v_1 through the squeezer, filter cavity and interferometer to the detection point,

$$\mathbf{T_1} = \tau_{\rm ro}\mathbf{T_{ifo}}(t_{00}\mathbf{T_{fc}} + \mathbf{T_{mm}})\mathbf{T_{inj}}. \tag{38}$$

We now consider the vacuum field v_2, which accounts for all fluctuations coupled into the beam due to injection losses, losses inside the filter cavity itself and imperfect mode matching. The audio-sideband transmission coefficient from the squeezer to the interferometer is

$$\tau_2(\Omega) = (t_{00}r_{\rm fc}(\Omega) + t_{\rm mm})\tau_{\rm inj}. \tag{39}$$

In the two-photon picture, the average of the upper and lower sideband losses gives the source term for the v_2 vacuum fluctuations, so that

$$\mathbf{T_2} = \tau_{\rm ro}\mathbf{T_{ifo}}\Lambda_2 \tag{40}$$

where

$$\Lambda_2 = \sqrt{1 - (|\tau_2(+\Omega)|^2 + |\tau_2(-\Omega)|^2)/2}. \tag{41}$$

Finally, frequency-independent losses $\Lambda_{\rm ro}^2$ between the interferometer and the readout introduce a second source of attenuation of the squeezed state and accompanying vacuum fluctuations v_3, a process described by the following transfer matrix and transmission coefficient

$$\mathbf{T_3} = \Lambda_{\rm ro}, \qquad \tau_{\rm ro} = \sqrt{1 - \Lambda_{\rm ro}^2}. \tag{42}$$

These losses cannot be added to the injection losses mentioned above since they are separated by the nonlinear effects of the interferometer. Explicitly, losses before and after the interferometer are not equivalent.

The single-sided power spectrum of the quantum noise at the interferometer readout is then given by

$$N(\zeta) = \underbrace{|\bar{\mathbf{b}}_\zeta \cdot \mathbf{T_1} \cdot v_1|^2}_{N_1(\zeta)} + \underbrace{|\bar{\mathbf{b}}_\zeta \cdot \mathbf{T_2} \cdot v_2|^2}_{N_2(\zeta)} + \underbrace{|\bar{\mathbf{b}}_\zeta \cdot \mathbf{T_3} \cdot v_3|^2}_{N_3(\zeta)}, \tag{43}$$

where the local oscillator field $\bar{\mathbf{b}}_\zeta = A_{\rm LO}(\sin\zeta \quad \cos\zeta)$, with amplitude $A_{\rm LO}$, determines the readout quadrature. All mathematical operations are as defined in [14] and ζ is defined such that $N(\zeta = 0)$ is the noise in the quadrature containing the interferometer signal.

We now investigate (43) more closely, providing analytical expressions for the contribution of each term. To improve readability, we normalize all noise powers with respect to shot noise (see Appendix A 2). This action is denoted through the use of an additional circumflex, i.e. $\widehat{N}$ rather than N.

1. Noise due to vacuum fluctuations passing through the squeezer, $\widehat{N}_1$

As the only term with dependence on filter cavity performance, examination of $\widehat{N}_1(\zeta)$ allows one to determine the optimal filter cavity parameters.

A comprehensive expression for $\widehat{N}_1(\zeta = 0)$ may be developed starting from (38). However, for clarity, and to assist in gaining physical understanding, we restrict our discussion to an optimally matched filter cavity, and neglect injection and readout losses, to obtain a simple description in terms of the optomechanical coupling constant $\mathcal{K}$, the cavity rotation angle α_p and reflectivities ρ_p and ρ_m. In this case,

$$\begin{aligned}\widehat{N}_1(\zeta = 0) = {}& (\rho_p^2 e^{-2\sigma} + \rho_m^2 e^{2\sigma})(\cos\alpha_p + \mathcal{K}\sin\alpha_p)^2\\ &+ (\rho_p^2 e^{2\sigma} + \rho_m^2 e^{-2\sigma})(\mathcal{K}\cos\alpha_p - \sin\alpha_p)^2.\end{aligned} \tag{44}$$

Equation (44) elucidates both the effect of a filter cavity and the role of filter cavity losses. We first remark that in

the absence of both squeezed light ($\sigma = 0$) and a filter cavity (equivalent to $\rho_p = 1$, $\rho_m = 0$) the interferometer output noise is simply

$$\widehat{N}_1 = 1 + \mathcal{K}^2. \tag{45}$$

With the addition of frequency-independent squeezed light ($\sigma \neq 0$, $\alpha_p = 0$), the total output noise becomes

$$\widehat{N}_1 = e^{-2\sigma} + e^{2\sigma}\mathcal{K}^2. \tag{46}$$

In the frequency region in which $\mathcal{K} < 1$ the noise is reduced by the presence of squeezed light but for $\mathcal{K} > 1$ the noise is degraded by the antisqueezing component $e^{2\sigma}$. Had we chosen $\alpha_p = \pi/2$ these roles would have been reversed.

The presence of a filter cavity ($\alpha_p = \alpha_p(\Omega) \neq 0$) allows one to minimize the impact of antisqueezing on the measured noise. For a lossless filter cavity ($\rho_m = 0$, $\rho_p = 1$) the antisqueezing can be completely nulled by selecting filter cavity parameters such that $\alpha_p = \arctan(\mathcal{K})$, giving the minimal quantum noise

$$\widehat{N}_1 = e^{-2\sigma}(1 + \mathcal{K}^2). \tag{47}$$

With the addition of filter cavity losses ($\rho_m \neq 0$) the total noise becomes

$$\widehat{N}_1 = (\rho_p^2 e^{-2\sigma} + \rho_m^2 e^{2\sigma})(1 + \mathcal{K}^2) \tag{48}$$

and there is no value of α_p for which the influence of antisqueezing can be completely nulled (due to the coherent dephasing effect discussed above in II B). It is important to highlight that precluding "optimal" rotation is not the only downside of a lossy filter cavity. Intracavity losses also introduce additional vacuum fluctuations, v_2, which do not pass through the squeezer, leading to increased noise in the interferometer readout via the T_2 transfer matrix. Considering an optimally mode-matched filter cavity, this effect is most noticeable in (41), which becomes simply $\Lambda_2 = \sqrt{1 - (\rho_p^2 + \rho_m^2)} \neq 0$ (see also Sec. II E 2 below).

For an interferometer in which $\gamma_{\rm ifo} \lesssim \Omega_{\rm SQL}$, like a power-recycled Michelson interferometer (or a detuned signal-recycled Michelson interferometer), a single filter cavity is not capable of realizing the desired rotation of the squeezed quadrature, as extensively described in Sec. V and Appendix C of [7]. Conversely, for a broadband interferometer like Advanced LIGO, in which $\gamma_{\rm ifo} > 5\Omega_{\rm SQL}$ and the approximation $\mathcal{K} \simeq (\Omega_{\rm SQL}/\Omega)^2$ holds, it can be shown, from (17) and (37), that the output noise is minimized by a single filter cavity with the following parameters

$$\Delta\omega_{\rm fc} = \sqrt{1 - \epsilon}\,\gamma_{\rm fc} \tag{49}$$

and

$$\gamma_{\rm fc} = \sqrt{\frac{2}{(2 - \epsilon)\sqrt{1 - \epsilon}}}\frac{\Omega_{\rm SQL}}{\sqrt{2}}, \tag{50}$$

from which the requirements for a lossless filter cavity ($\epsilon = 0$) can be derived,

$$\Delta\omega_{\rm fc} = \gamma_{\rm fc} \tag{51}$$

and

$$\gamma_{\rm fc} = \frac{\Omega_{\rm SQL}}{\sqrt{2}}. \tag{52}$$

In practice, for fixed cavity length and losses, the value of $t_{\rm in}$ is tuned to obtain the required filter cavity bandwidth. However, changing $t_{\rm in}$ affects both ϵ and $\gamma_{\rm fc}$, making (50) inconvenient to solve. Nevertheless, equating the right-hand side of (50) with the expression for $\gamma_{\rm fc}$ derived from (8), one obtains a version of ϵ which is independent of $t_{\rm in}$,

$$\epsilon = \frac{4}{2 + \sqrt{2 + 2\sqrt{1 + \left(\frac{2\Omega_{\rm SQL}}{f_{\rm FSR}\Lambda_{\rm rt}^2}\right)^4}}}, \tag{53}$$

and can be used to find $\Delta\omega_{\rm fc}$ and $\gamma_{\rm fc}$. Then, from (10),

$$t_{\rm in}^2 = \frac{2\gamma_{\rm fc}}{f_{\rm FSR}} - \Lambda_{\rm rt}^2. \tag{54}$$

We note that as filter cavity losses increase, the ideal filter cavity bandwidth also increases, while the optimal cavity detuning is reduced. As a consequence, the desired value of $t_{\rm in}$ is approximately constant for $\epsilon \lesssim 0.3$.

2. Noise due to vacuum fluctuations which do not pass through the squeezer, $\widehat{N}_2$

Let us now consider $\widehat{N}_2(\zeta = 0)$, the term describing noise due to loss-induced vacuum fluctuations which do not pass through the squeezer. Assuming perfect mode matching, Λ_2 from (41) can be written as

$$\Lambda_2 = \sqrt{1 - \tau_{\rm inj}^2(\rho_p^2 + \rho_m^2)}. \tag{55}$$

Thus, using (40), we obtain

$$\begin{aligned}\widehat{N}_2(\zeta = 0) &= \tau_{\rm ro}^2(1 + \mathcal{K}^2)\Lambda_2^2 \\ &= \tau_{\rm ro}^2(1 + \mathcal{K}^2)(1 - \tau_{\rm inj}^2(\rho_p^2 + \rho_m^2)).\end{aligned} \tag{56}$$

3. Noise due to vacuum fluctuations in the readout, $\widehat{N}_3$

The noise due to vacuum fluctuations entering at the interferometer readout follows trivially from (42),

$$\widehat{N}_3(\zeta = 0) = \Lambda_{\rm ro}^2 = 1 - \tau_{\rm ro}^2. \tag{57}$$

F. Phase noise

In addition to optical losses and mode mismatch, a further cause of squeezing degradation is phase noise, also referred to as "squeezed quadrature fluctuations" [13]. In this section we develop a means of quantifying the impact of this important degradation mechanism.

Assuming some parameter X in $\mathbf{T_1}$ or $\mathbf{T_2}$ has small, Gaussian-distributed fluctuations with variance δX^2, the average readout noise is given by

$$\widehat{N}_{\mathrm{avg}}(\zeta) \simeq \widehat{N}(\zeta, X) + \frac{\partial^2 \widehat{N}(\zeta, X)}{\partial X^2}\frac{\delta X^2}{2} \tag{58}$$

$$\simeq \frac{\widehat{N}(\zeta, X+\delta X) + \widehat{N}(\zeta, X-\delta X)}{2}. \tag{59}$$

Extending this approach to multiple incoherent noise parameters X_n yields

$$\widehat{N}_{\mathrm{avg}} \simeq \widehat{N} + \sum_n \frac{\partial^2 \widehat{N}(X_n)}{\partial {X_n}^2}\frac{\delta X_n^2}{2} \tag{60}$$

$$\simeq \widehat{N} + \sum_n \left(\frac{\widehat{N}(X_n+\delta X_n) + \widehat{N}(X_n-\delta X_n)}{2} - \widehat{N}\right), \tag{61}$$

where the parameters not explicitly listed as arguments to $\widehat{N}$, including ζ, are assumed to take on their mean values.

While (61) is sufficient to evaluate $\widehat{N}_{\mathrm{avg}}$ for any collection of phase noise sources, we choose to follow the same approach adopted in the treatment of optical losses, considering two classes of squeezed quadrature fluctuations: extra-cavity fluctuations that are frequency independent and intracavity fluctuations that are frequency dependent.

Examples of frequency-independent phase noise sources include length fluctuations in the squeezed field injection path and instabilities in the relative phase of the local oscillator or the radio-frequency sidebands which co-propagate with the squeezed field. Such frequency-independent noise may be represented by variations, $\delta\zeta$, in the homodyne readout angle ζ.

Frequency-dependent phase noise is caused by variability in the filter cavity detuning $\Delta\omega_{\mathrm{fc}}$ [see (4)]. This detuning noise results from filter cavity length noise δL_{fc}, driven by seismic excitation of the cavity mirrors or sensor noise associated with the filter cavity length control loop, according to

$$\delta\Delta\omega_{\mathrm{fc}} = \frac{\omega_0}{L_{\mathrm{fc}}}\delta L_{\mathrm{fc}}. \tag{62}$$

Detuning noise gives rise to frequency-dependent phase noise through the properties of the filter cavity resonance. For example, the dependence of $\mathbf{T_{fc}}$ on $\Delta\omega_{\mathrm{fc}}$ is weak for $\Omega \gg \Delta\omega_{\mathrm{fc}}$, i.e. for frequencies far from resonance, and stronger for $\Omega \simeq \Delta\omega_{\mathrm{fc}}$, i.e. for frequencies close to resonance.

General analytic expressions for $\widehat{N}_{\mathrm{avg}}$ as a function of $\delta\zeta$ and δL_{fc} are neither concise nor especially edifying. Therefore, in the following section, we apply (61) numerically to illustrate the impact of phase noise in a typical advanced gravitational-wave detector.

III. A 16 M FILTER CAVITY FOR ADVANCED LIGO

We now apply the analytical model expounded above to the particular case of a 16 m filter cavity. Such a system has recently been considered for application to Advanced LIGO [14] and therefore we use the specifications of this interferometer in our study (see Table I).

The remaining parameters, show in Table II, represent what we believe is technically feasible using currently available technology. For example, the filter cavity length noise estimate δL_{fc} assumes that the cavity mirrors will be held in single-stage suspension systems located on seismically isolated HAM-ISI tables [19] and that the filter cavity length control loop will have 150 Hz unity gain frequency, and while a 2% mode mismatch between the squeezed field and the filter cavity is extremely small, newly developed actuators [20,21] allow us to be optimistic. We chose to inject 9.1 dB of squeezing into our system as this value results in 6 dB of high-frequency squeezing at the interferometer readout (a goal for second-generation interferometers [5]) and, conservatively, to

TABLE II. Parameters used in the application of our model to Advanced LIGO.

Parameter	Symbol	Value
Filter cavity length	L_{fc}	16 m
Filter cavity half-bandwidth	γ_{fc}	$2\pi \times 61.4$ Hz
Filter cavity detuning	$\Delta\omega_{\mathrm{fc}}$	$2\pi \times 48$ Hz
Filter cavity input mirror transmissivity	t_{in}^2	66.3 ppm
Filter cavity losses	Λ_{rt}^2	16 ppm
Injection losses	Λ_{inj}^2	5%
Readout losses	Λ_{ro}^2	5%
Mode-mismatch losses (squeezer-filter cavity)	$\Lambda_{\mathrm{mmFC}}^2$	2%
Mode-mismatch losses (squeezer-local oscillator)	$\Lambda_{\mathrm{mmLO}}^2$	5%
Frequency-independent phase noise (RMS)	$\delta\zeta$	30 mrad
Filter cavity length noise (RMS)	δL_{fc}	0.3 pm
Injected squeezing	σ_{dB}	9.1 dB

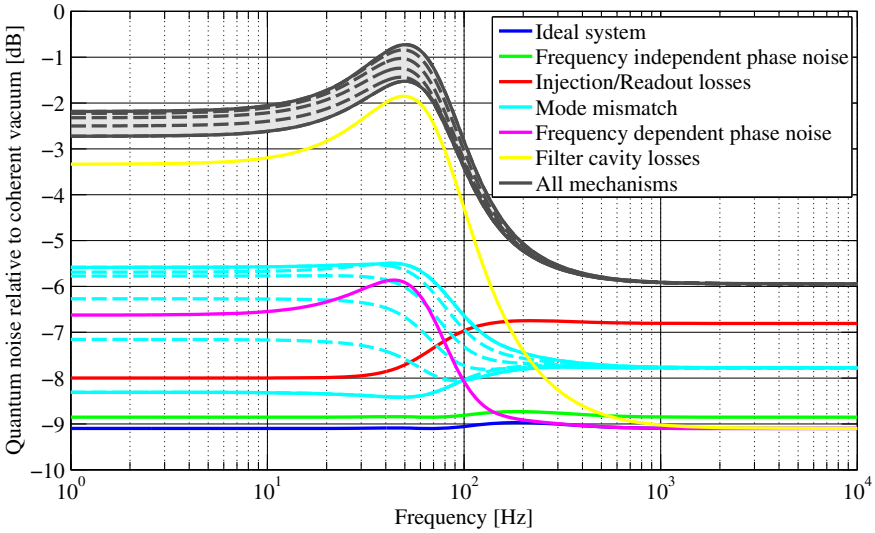

FIG. 2 (color online). Power spectral density of quantum noise in the signal quadrature relative to coherent vacuum. Traces show how the noise reduction of a −9.1 dB minimum uncertainty squeezed state is impaired by each of the various decoherence and degradation mechanisms discussed herein. The effects of coherent dephasing are included in the "Filter cavity losses" trace. The family of "Mode mismatch" curves encapsulates the unknown phase of t_{mm}, with solid curves defining upper and lower bounds for the induced noise [see Sec. II C, specifically (25)]. The trace labelled "All mechanisms" illustrates the total impact when the contributions of all decoherence and degradation effects are considered simultaneously.

consider a filter cavity with 16 ppm round-trip loss, even if recent investigations have shown that lower losses are achievable [22].

The results of our investigation are shown in Fig. 2. One observes that intracavity losses are the dominant source of decoherence below ∼300 Hz. However, we note that, with small changes in parameter choice, the impact of the other coupling mechanisms could also become important. For instance, filter cavity length fluctuations approaching 1 pm RMS would greatly compromise low frequency performance.

At higher frequencies, injection, readout and mode-mismatch losses are the most influential effects. With total losses of ∼15%, measuring 6 dB of squeezing demands that more than 9 dB be present at the injection point.

Even under the idealized condition of negligible filter cavity losses ($\Lambda_{\mathrm{rt}}^2/L_{\mathrm{fc}} \ll 1$ ppm/m), achieving a broadband improvement greater than 6 dB places extremely stringent requirements on the mode matching throughout the system and on the filter cavity length noise.

IV. CONCLUSIONS

Quantum filter cavities were proposed several years ago as means of maximizing the benefit available from squeezing in advanced interferometric gravitational-wave detectors [7]. However, the technical noise sources which practically limit filter cavity performance have, until now, been neglected. In this paper we have presented an analytical model capable of quantifying the impact of several such noise sources, including optical loss, mode mismatch and frequency-dependent phase noise. We find that real-world decoherence and degradation can be significant and therefore must be taken into account when evaluating the overall performance of a filter cavity. Applying our model to the specific case of Advanced LIGO [14], we conclude that a 16 m filter cavity, built with currently available technology, offers considerable performance gains and remains a viable and worthwhile near-term upgrade to the generation of gravitational-wave detectors presently under construction.

ACKNOWLEDGMENTS

The authors gratefully acknowledge the support of the National Science Foundation and the LIGO Laboratory, operating under cooperative Agreement No. PHY-0757058. This paper has been assigned LIGO Document No. LIGO-P1400018.

APPENDIX A: FORMALISM

In this appendix we place the calculations presented above in the context of the one-photon and two-photon formalisms extensively discussed in literature (see e.g. [12,18]). We commence by connecting the one-photon expression for the time-varying part of the electromagnetic field to power fluctuations on a photo-detector. We then transform the derived expression into the two-photon basis to explicitly show how vacuum fluctuations

generate measurable noise. This calculation is subsequently generalized to the case of multiple vacuum fields arriving at a photo-detector after having propagated through an optical system, revealing the origin of (43). Finally, we discuss how quantum noise may be calculated for systems best described in the one-photon picture, in the process deriving the one-photon to two-photon conversion matrix (11).

1. One-photon and two-photon in context

The one-photon and two-photon formalisms provide two alternative ways of expressing fields. In the one-photon formalism, as described by (2.6) of [18], the time varying part of the electromagnetic field $E(t)$ is written in terms of its audio-sideband components around the carrier frequency ω_0,

$$\begin{aligned} E(t) &= \sqrt{\frac{2\pi\hbar\omega_0}{\mathcal{A}c}} e^{-i\omega_0 t} \int_0^{+\infty} [a_+(\Omega)e^{-i\Omega t} + a_-(\Omega)e^{i\Omega t}] \frac{d\Omega}{2\pi} + \text{H.c.} \\ &= \sqrt{\frac{2\pi\hbar\omega_0}{\mathcal{A}c}} \cdot 2\text{Re}\left[e^{-i\omega_0 t} \int_0^{+\infty} [a_+(\Omega)e^{-i\Omega t} + a_-(\Omega)e^{i\Omega t}] \frac{d\Omega}{2\pi} \right], \end{aligned} \tag{A1}$$

where $\mathcal{A}$ is the "effective area", "H.c." means Hermitian conjugate and $a_\pm(\Omega)$ are the normalized amplitudes of the upper and lower sidebands at frequencies $\omega_0 \pm \Omega$ in dimensions of $(\text{number of photons/Hz})^{1/2}$ (see [10] for greater detail).

By introducing $\mathcal{E}_0$ defined as

$$\mathcal{E}_0 = \sqrt{\frac{2}{\mathcal{A}c\epsilon_0}}, \tag{A2}$$

and noting that [18] uses $\epsilon_0 = 1/4\pi$, $E(t)$ can be rewritten as

$$E(t) = \mathcal{E}_0 \sqrt{\hbar\omega_0} \text{Re}\left[e^{-i\omega_0 t} \int_0^{+\infty} [a_+(\Omega)e^{-i\Omega t} + a_-(\Omega)e^{i\Omega t}] \frac{d\Omega}{2\pi} \right] = \text{Re}[\mathcal{E}_0 \delta A(t) e^{-i\omega_0 t}] \tag{A3}$$

where we have introduced the time-dependent amplitude

$$\delta A(t) = \sqrt{\hbar\omega_0} \int_0^{+\infty} [a_+(\Omega)e^{-i\Omega t} + a_-(\Omega)e^{i\Omega t}] \frac{d\Omega}{2\pi}. \tag{A4}$$

In our application these fluctuations arrive to the photo-detector together with a strong, constant *local oscillator* field A_0 such that

$$E(t) = \text{Re}[\mathcal{E}_0(A_0 + \delta A(t))e^{-i\omega_0 t}]. \tag{A5}$$

The power $P(t)$ transported by the beam can then be written as

$$\begin{aligned} P(t) &= \mathcal{A}\overline{I(t)} = \mathcal{A}c\epsilon_0 \overline{E(t)^2} = \frac{\mathcal{A}c\epsilon_0}{2} |\mathcal{E}_0(A_0 + \delta A(t))|^2 \\ &= |A_0|^2 + 2\text{Re}[A_0^* \delta A(t)] + |\delta A(t)|^2, \end{aligned} \tag{A6}$$

where $I(t)$ denotes intensity and the overbar indicates the average over one or more cycles of the electromagnetic wave. Note that the effective area $\mathcal{A}$ has cancelled and does not have a meaningful effect on the measurable power. Since $\delta A(t) \ll A_0$, we can approximate the power fluctuation $\delta P(t)$ as

$$\delta P(t) \equiv P(t) - |A_0|^2 \simeq 2\text{Re}[A_0^* \delta A(t)]. \tag{A7}$$

Switching to the frequency domain, we take the Fourier transform of $\delta P(t)$ to find

$$\begin{aligned} \delta\tilde{P}(\Omega) &= \int_{-\infty}^{+\infty} 2\text{Re}[A_0^* \delta A(t)] e^{i\Omega t} dt \\ &= \int_{-\infty}^{+\infty} [A_0^* \delta A(t) + A_0 \delta A^*(t)] e^{i\Omega t} dt \\ &= A_0^* \delta\tilde{A}(\Omega) + A_0 \delta\tilde{A}^*(-\Omega) \\ &= \sqrt{\hbar\omega_0}[A_0^* a_+(\Omega) + A_0 a_-^*(\Omega)], \end{aligned} \tag{A8}$$

where, in the final step, we have used (A4).

The two-photon formalism defines quadrature fields as linear combinations of the one-photon fields [18],

$$a_1 = \frac{(a_+ + a_-^*)}{\sqrt{2}} \quad \text{and} \quad a_2 = \frac{(a_+ - a_-^*)}{\sqrt{2}i} \tag{A9}$$

such that

$$a_+ = \frac{(a_1 + ia_2)}{\sqrt{2}} \quad \text{and} \quad a_-^* = \frac{(a_1 - ia_2)}{\sqrt{2}}. \tag{A10}$$

By substituting (A10) into (A8), we obtain the frequency-domain expression for δP in the two-photon formalism,

$$\delta\tilde{P}(\Omega) = \sqrt{\hbar\omega_0/2}[(A_0^* + A_0)a_1(\Omega) + i(A_0^* - A_0)a_2(\Omega)] = \sqrt{2\hbar\omega_0}[\mathrm{Re}[A_0]a_1(\Omega) + \mathrm{Im}[A_0]a_2(\Omega)]. \quad \text{(A11)}$$

Expressing the local oscillator's amplitude and phase explicitly, $A_0 = A_{\mathrm{LO}}e^{i\phi}$, $\delta\tilde{P}(\Omega)$ becomes

$$\delta\tilde{P}(\Omega) = \sqrt{2\hbar\omega_0}A_{\mathrm{LO}}[a_1(\Omega)\cos\phi + a_2(\Omega)\sin\phi]. \quad \text{(A12)}$$

2. Calculation of quantum noise

Equation (A12) provides a simple method of calculating the power fluctuations on a photo-detector given any time-varying electromagnetic field beating against a local oscillator.

As a specific and relevant example, quantum noise (due to the zero-point energy of the electromagnetic field) drives vacuum fluctuations, $a_1(\Omega)$ and $a_2(\Omega)$, which are incoherent and of unit amplitude at all frequencies. The resulting noise power generated is

$$N = |\delta\tilde{P}|^2 = 2\hbar\omega_0 A_{\mathrm{LO}}^2(|a_1\cos\phi|^2 + |a_2\sin\phi|^2) \quad \text{(A13)}$$

$$= 2\hbar\omega_0 A_{\mathrm{LO}}^2, \quad \text{(A14)}$$

where a_1 and a_2 have initially been listed explicitly to highlight the incoherent nature of the noise associated with each of the two quadratures. Note that this expression is consistent with the familiar equation $\sqrt{2P_{\mathrm{avg}}h\nu}$ for the amplitude spectral density of shot noise, since the average power level P_{avg} is equal to A_{LO}^2.

The tools of linear algebra can now be exploited to simplify these expressions, allowing one to rewrite the noise as

$$N = \left| A_{\mathrm{LO}}(\cos\phi \quad \sin\phi) \cdot \sqrt{2\hbar\omega_0}\begin{pmatrix} 1 & 0 \\ 0 & 1 \end{pmatrix}\right|^2 = |\bar{\mathbf{b}}_\zeta \cdot v_{\mathrm{in}}|^2, \quad \text{(A15)}$$

where the local oscillator is as defined in Sec. II E (given the LO phase convention $\zeta = \pi/2 - \phi$),

$$\bar{\mathbf{b}}_\zeta = A_{\mathrm{LO}}(\sin\zeta \quad \cos\zeta) = A_{\mathrm{LO}}(\cos\phi \quad \sin\phi), \quad \text{(A16)}$$

and v_{in}, simply proportional to the 2×2 identity matrix, embodies the two independent vacuum noise sources

$$v_{\mathrm{in}} = \sqrt{2\hbar\omega}\mathbf{I}. \quad \text{(A17)}$$

In general, to calculate the quantum noise in an optical system, the vacuum field v_{in} entering an open port is propagated to the readout photodetector through the transfer matrix $\mathbf{T}$ of the system

$$v_{\mathrm{out}} = \mathbf{T}\cdot v_{\mathrm{in}}, \quad \text{(A18)}$$

as described in [14]. The vacuum fluctuations v_{out} then beat against the local oscillator field present on the photodetector to give the power spectrum of quantum noise

$$N = |\bar{\mathbf{b}}_\zeta \cdot v_{\mathrm{out}}|^2 = |\bar{\mathbf{b}}_\zeta \cdot \mathbf{T}\cdot v_{\mathrm{in}}|^2. \quad \text{(A19)}$$

If multiple paths lead to the same photodetector, the total noise may be calculated as the sum of the contributions due to each vacuum source,

$$N = \sum_n |\bar{\mathbf{b}}_\zeta \cdot \mathbf{T}_n \cdot v_n|^2 = 2\hbar\omega_0 \sum_n |\bar{\mathbf{b}}_\zeta \cdot \mathbf{T}_n|^2. \quad \text{(A20)}$$

Finally, dividing by the shot noise level gives the normalized noise power used throughout this paper

$$\widehat{N} = \frac{N}{2\hbar\omega_0 A_{\mathrm{LO}}^2}. \quad \text{(A21)}$$

3. One-photon transfer

Some optical systems, like filter cavities, are better described by the one-photon formalism, as this makes their transfer matrices diagonal. As in the two-photon formalism, the quantum noise N is the result of the incoherent sum of the noise generated by two vacuum fields. Although, in this case, the fields of concern are a_+ and a_- (rather than a_1 and a_2). Beginning from (A8), the resulting noise is

$$N = |\delta\tilde{P}|^2 = \hbar\omega_0(|A_0^* a_+|^2 + |A_0 a_-|^2) = 2\hbar\omega_0 A_{\mathrm{LO}}^2, \quad \text{(A22)}$$

where, as before, a_+ and a_- have been included explicitly before being set to unity.

However, rather than develop an equivalent set of linear algebra expressions for computing total noise output in the one-photon formalism, we instead use (A9) and (A10) to define a one-photon to two-photon conversion matrix

$$\mathbf{A_2} = \frac{1}{\sqrt{2}}\begin{pmatrix} 1 & 1 \\ -\mathrm{i} & +\mathrm{i} \end{pmatrix} \quad \text{such that} \quad \begin{pmatrix} a_1 \\ a_2 \end{pmatrix} = \mathbf{A_2}\begin{pmatrix} a_+ \\ a_-^* \end{pmatrix}. \quad \text{(A23)}$$

The one-photon transfer matrix of any optical system which does not mix upper and lower audio sidebands (i.e. any linear system) can then be expressed in the two-photon formalism as

$$\mathbf{T} = \mathbf{A_2}\cdot\begin{pmatrix} t_+ & 0 \\ 0 & t_-^* \end{pmatrix}\cdot \mathbf{A_2}^{-1}, \quad \text{(A24)}$$

where $t_\pm$ are the transfer coefficients for the upper and lower audio sidebands.

[1] S. Takeda, T. Mizuta, M. Fuwa, P. van Loock, and A. Furusawa, Nature (London) **500**, 315 (2013).
[2] M. A. Taylor, J. Janousek, V. Daria, J. Knittel, B. Hage, H.-A. Bachor, and W. P. Bowen, Nat. Photonics **7**, 229 (2013).
[3] H. Yonezawa, D. Nakane, T. A. Wheatley, K. Iwasawa, S. Takeda, H. Arao, K. Ohki, K. Tsumura, D. W. Berry, T. C. Ralph, H. M. Wiseman, E. H. Huntington, and A. Furusawa, Science **337**, 1514 (2012).
[4] The LIGO Scientific Collaboration, Nat. Phys. **7**, 962 (2011).
[5] The LIGO Scientific Collaboration, Nat. Photonics **7**, 613 (2013).
[6] G. M. Harry and the LIGO Scientific Collaboration, Classical Quantum Gravity **27**, 084006 (2010).
[7] H. J. Kimble, Y. Levin, A. B. Matsko, K. S. Thorne, and S. P. Vyatchanin, Phys. Rev. D **65**, 022002 (2001).
[8] J. Harms, Y. Chen, S. Chelkowski, A. Franzen, H. Vahlbruch, K. Danzmann, and R. Schnabel, Phys. Rev. D **68**, 042001 (2003).
[9] S. Chelkowski, H. Vahlbruch, B. Hage, A. Franzen, N. Lastzka, K. Danzmann, and R. Schnabel, Phys. Rev. A **71**, 013806 (2005).
[10] C. M. Caves and B. L. Schumaker, Phys. Rev. A **31**, 3068 (1985).
[11] B. L. Schumaker and C. M. Caves, Phys. Rev. A **31**, 3093 (1985).
[12] T. Corbitt, Y. Chen, and N. Mavalvala, Phys. Rev. A **72**, 013818 (2005).
[13] S. Dwyer, Ph.D. thesis, Massachusetts Institute of Technology, 2013.
[14] M. Evans, L. Barsotti, P. Kwee, J. Harms, and H. Miao, Phys. Rev. D **88**, 022002 (2013).
[15] Our model treats all injection losses as occurring before the filter cavity. This approach is valid as the action of the filter cavity on coherent vacuum states is null.
[16] Note that the ϵ defined here is similar to that in Eq. (94) of [7], and that $\epsilon \to 1$ for an optimally coupled cavity.
[17] F. Y. Khalili, Phys. Rev. D **81**, 122002 (2010).
[18] A. Buonanno and Y. Chen, Phys. Rev. D **64**, 042006 (2001).
[19] M. Evans (LIGO Scientific Collaboration), Tech. Rep. T1200155, 2012.
[20] M. Kasprzack, B. Canuel, F. Cavalier, R. Day, E. Genin, J. Marque, D. Sentenac, and G. Vajente, Appl. Opt. **52**, 2909 (2013).
[21] Z. Liu, P. Fulda, M. A. Arain, L. Williams, G. Mueller, D. B. Tanner, and D. H. Reitze, Appl. Opt. **52**, 6452 (2013).
[22] T. Isogai, J. Miller, P. Kwee, L. Barsotti, and M. Evans, Opt. Express **21**, 30114 (2013).